Solid Solubility, Raman Spectra and Electrical Property of the Solid Solutions $Ce_{1-x}Nd_xO_{2-\delta}$ by Sol-gel Route

LIN, Xiao-Min* (林晓敏) **LI, Li-Ping**(李莉萍) **LI, Guang-She**†(李广社)
SU, Wen-Hui(苏文辉)

Physics Department and Key Laboratory of Inorganic Synthesis and Preparative Chemistry, Jilin University, Changchun, Jilin 130023, China

$Ce_{1-x}Nd_xO_{2-\delta}$ (x = 0.05—0.55) solid solutions prepared by sol-gel route were crystallized in a cubic fluorite structure. The solid limit was determined to be as high as x = 0.45. Raman spectra of the solid solutions with lower composition exhibited only one band, which was assigned to F_{2g} mode. Increasing composition produced broad and asymmetric F_{2g} mode with an appearance of low frequency tail. The new broad peak observed at higher frequency side of the F_{2g} mode associated with the oxygen vacancy in the lattice. The impedance spectra of the solid solutions showed definitely ionic conduction, and $Ce_{0.80}Nd_{0.20}O_{2-\delta}$ solid solution possessed a maximum conductivity. At 500 ℃, the conductivity and activation energy were 2.65×10^{-3} S/cm and 0.82 eV, respectively.

Keywords $Ce_{1-x}Nd_xO_{2-\delta}$, Raman spectrum, ionic conductivity

Introduction

Preparation of solid electrolytes containing rare earth metals is a key point for solid-state electrochemical applications.[1] In the last decades, several solid electrolytes were developed such as ceria doped with divalent or trivalent ions to further increase the efficiency of the electrochemical device and to decrease the operation temperature. This is because ceria-based solid solutions doped with lower valence ions usually possess conductivity much higher than yttrium-stabilized zirconia (YSZ).[2] The ionic conductivity for ceria-based electrolytes is strongly dependent on the oxygen vacancy content, which can be effectively adjusted by doping aliovalent ions or reducing valence of cerium ions.[3] The charge compensation when introducing lower valence ions in ceria lattice might be achieved by producing oxygen vacancy (extrinsic vacancy). The previous studies have shown some percentages of intrinsic oxygen vacancies in ceria lattice arising from the reduction equilibrium of Ce^{4+}/Ce^{3+}, which can much improve the ionic conduction.[4] Soft chemistry routes often yield new solid solutions having controllable valence states and defects. We have recently obtained very high solid solubility and excellent ionic conductivity in ceria based solid solutions by hydrothermal condition.[2] In this paper, we report the results about the preparation of $Ce_{1-x}Nd_xO_{2-\delta}$ solid solutions by sol-gel route, the determination of the solid solubility, and the discussion of Raman spectra, oxygen vacancy and ionic conductivity.

Experimental

The solid solutions were prepared by sol-gel route using $Ce(NO_3)_3 \cdot 6H_2O$ and Nd_2O_3 as the starting materials. Firstly, the mixture of $Ce(NO_3)_3 \cdot 6H_2O$ and Nd_2O_3 with a molar ratio of Ce : Nd = $(1-x) : x$ (x = 0.05, 0.75, 0.10, 0.125, 0.15, 0.20, 0.30, 0.35, 0.40, 0.45, 0.50, 0.55) was dissolved into 5 mL of 1 mol/L nitrate solution. The citric acid was added in dropwise

* E-mail: linxiaomin@hotmail.com.
Received August 29, 2000; revised January 11, 2001; accepted March 5, 2001.
Project supported by the National Natural Science Foundation of China (No.19804005).
† Present address: *Research Center of Supercritical Fluid Technology, Tohoku University, Sendai* 980-8579, *Japan* (E-mail: guangshe@scf.che.tohoku.ac.jp).

into the mixture while stirring. The concentration of citric acid was controlled as the ratio of rare earth : citric acid = 1 : 1.2. The wet gel was formed after the solution was mixed with magnetically stirring at 80 ℃ for ca. 6 h. The dry gel obtained after baking the wet gel at 150 ℃ for 2 h was sintered at 800 ℃ in air for 10 h. The products were then pressed into $\phi 13 \times 1$ mm pellet under a pressure of 8 MPa and sintered at 1100 ℃ for 10 h.

The structures for the solid solutions were identified by powder X-ray diffraction (XRD) on a Rigaku, D/max-γA 12 kW XRD diffractometer (Cu K_α radiation) at room temperature. The lattice parameters for the samples were refined by least-squares method.

Raman spectra for the solid solutions were recorded using a J-YT64000 spectrometer with an Ar^+-ion laser. The excitation wavenumber employed is 488 nm. The resolution is 1 cm^{-1}. Elemental analysis was performed by energy dispersive X-ray analysis (EDX) using Electronic Microcopy (H-8100IV transition electronic microcopy) under an accelerated voltage of 200 kV. The molar ratios of Nd to Ce in the resulting solid solutions were closely near to the initial ones.

The opposite sides of the pellet samples were coated with silver paste and heated to 550 ℃ in air for half an hour so as to remove completely the organic components in the paste. The ionic conductivities for the pellet samples were measured using Solarton 1260 impedance/gain-phase analyzer with the alternating current having a frequency between 5 Hz and 3.1 MHz with the amplitude of 50 mV in the temperature range of 350—750 ℃ in air.

Results and discussion

XRD patterns for the samples obtained by sintering the dry gels at 800 ℃ are shown in Fig. 1. All diffraction peaks were highly symmetric and matched well with the diffraction data for standard fluorite structure. No XRD peaks for the component oxide Nd_2O_3 were detected ($x \leqslant 0.45$). This result confirmed the formation of $Ce_{1-x}Nd_xO_{2-\delta}$ solid solutions. At higher composition ($x > 0.45$) the separation of a second phase based on Nd_2O_3 was observed in the magnified X-ray patterns. XRD data shown in Fig. 1 were indexed in a cubic symmetry. The relationship between lattice parameter and composition x is shown in Fig. 2. The lattice parameters of all doped solid solutions were larger than the lattice parameter (0.5413 nm) of pure ceria (JCPDS, 34-394). With increasing composition the lattice parameters increased, that is in good agreement with effective ionic radii consideration which effective ionic radius of Nd^{3+} ions (0.1249 nm) is larger than that (0.111 nm) of Ce^{4+} ions.[5] When the composition was higher than $x = 0.45$, the lattice parameters kept near the same. This result may be related to the oxygen vacancy V_O, the localized defect associations and solubility limit. In the ceria-based solid solutions $Ce_{1-x}Nd_xO_{2-\delta}$, every two Nd^{3+} dopants or Ce^{3+} ions from reduction equilibrium, Ce^{4+}/Ce^{3+}, will generate one oxygen vacancy V_O,[2] the influence of oxygen vacancy on the lattice parameter is in

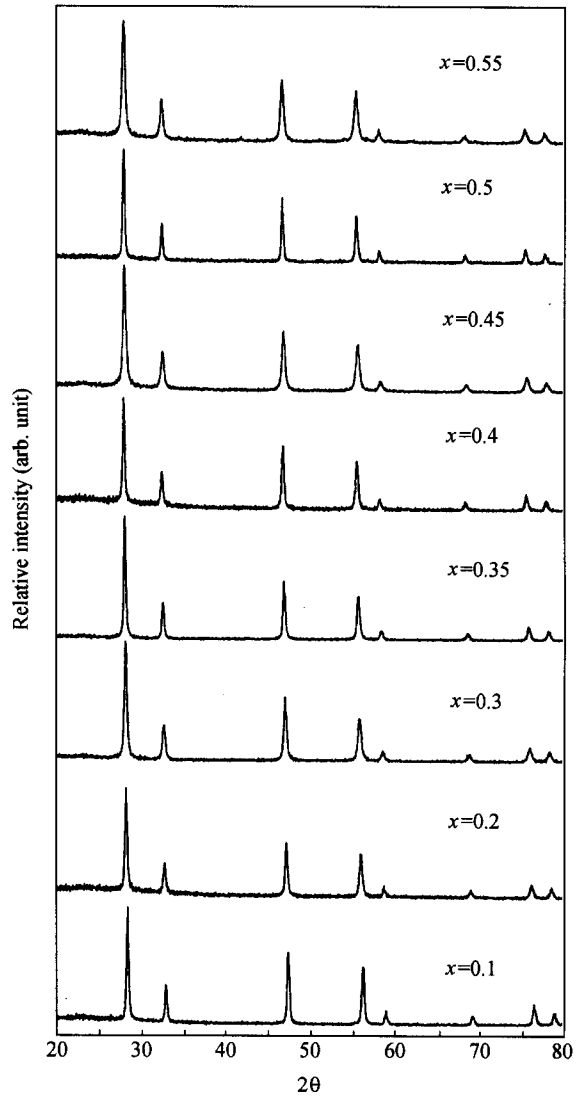

Fig. 1 XRD patterns of $Ce_{1-x}Nd_xO_{2-\delta}$ (x = 0.10—0.55) solid solutions obtained by sintering the dry gel at 800℃ for 10 h.

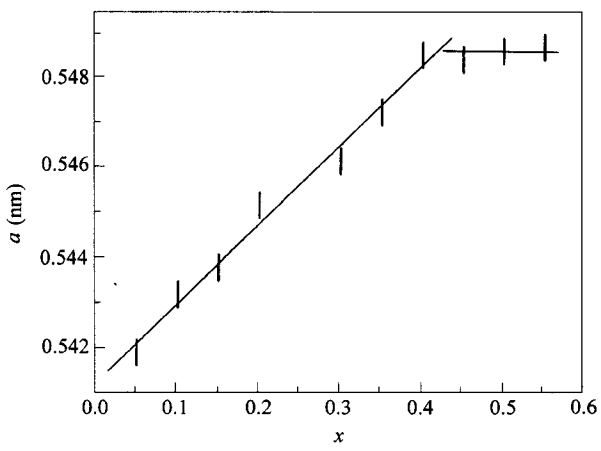

Fig. 2 Dependence of lattice parameter upon dopant content of $Ce_{1-x}Nd_xO_{2-\delta}$ solid solutions.

an opposite way to that of ionic radii. On the other hand, in the doped fluorite lattice there exist some changes of the relative contents of the oxygen vacancy V_O and the localized defect associations[3,4] (*e. g.*, $\{Nd_{Ce}\ V_O\}$ and $\{Ce_{Ce}\ V_O\}$ for the solutions of $Ce_{1-x}Nd_xO_{2-\delta}$. With the increasing composition, the number of oxygen vacancy V_O in the solutions will first increase with composition, and reach a maximum at certain dopant content x, then the defect associations begin to form.[3] When $x < 0.4$ the change of lattice parameter is mainly decided by the increasing of effective ionic size. However, when $x > 0.4$, the influence of oxygen vacancy and the localized defect associations may become predominant. In addition to the ionic size, oxygen vacancy content, and defect associations, the solid solubility is another important factor.[6] The previous studies have shown that rare earth oxides are highly soluble in ceria lattice.[7,8] The lattice parameter of doped ceria should follow the Vegard's rule, a linear relationship between lattice parameter and composition. The solubility limit can be determined from the intersection between the Vegard line and the horizontal line for the saturated value. In the solid solutions, the solid limit is as high as $x = 0.45$. It is far larger than $x = 0.20$ for $Ce_{1-x}Eu_xO_{2-\delta}$ solutions by hydrothermal conditions.[9] X-ray diffraction (Fig. 3) shows no transformation of the fluorite structure nor precipitation phase of Nd_2O_3 in solid solutions $Ce_{1-x}Nd_xO_{2-\delta}$ (x = 0.1—0.45) after sintering at 1100 ℃ for 10 h.

Ceria crystallizes in cubic fluorite structure with the space group $O_m^5(F_m3_m)$. Group theory analysis of such a crystal symmetry predicts one triply degenerate Raman active optical phonon of Γ_{25} symmetry (F_{2g}) and two infrared active phonons of Γ_{15} symmetry (F_{1u}), corresponding to the LO and TO modes.[10] Therefore, the first-order Raman spectrum of CeO_2 often shows only one Raman line. The Raman spectra for the present $Ce_{1-x}Nd_xO_{2-\delta}$ solid solutions are shown in Fig. 4. It can be seen that only F_{2g} mode is observed at ca. 465 cm^{-1} for lower composition. However, with increasing x, the F_{2g} mode became broad and asymmetric with the appearance of a frequency tail. It is worth to note that a new broad peak appeared on higher frequency side of the F_{2g} mode. This peak was closely related to the oxygen vacancy in the lattice.[11] With increasing dopant content, the Raman shift for F_{2g} mode remained the same. This result can be understood on the basis of the facts that F_{2g} band corresponds to the symmetric breathing mode of the oxygen atoms around the framework ions, and the mode frequency is nearly independent on cation mass.[12] The dilation of lattice can cause red shifting of mode frequency while increasing of oxygen vacancy content leads to blue shift.[11] The total consequence gives no obvious

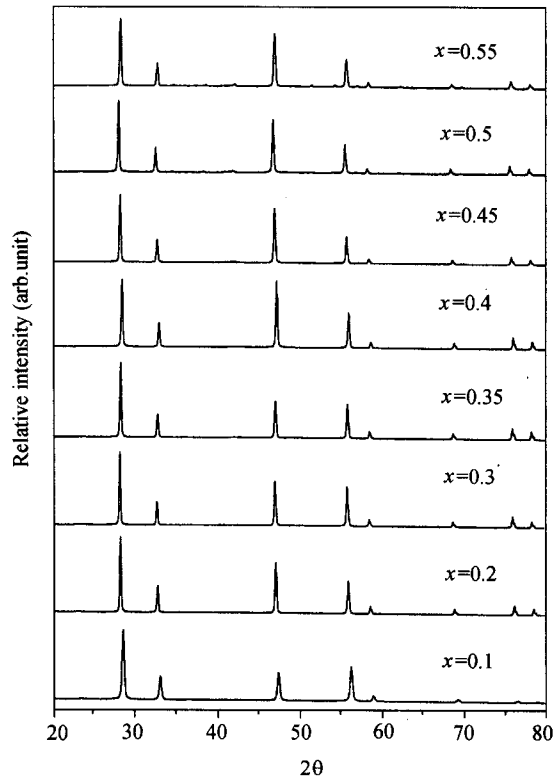

Fig. 3 XRD patterns of $Ce_{1-x}Nd_xO_{2-\delta}$ (x = 0.10—0.55) solid solutions obtained by sintering the dry gel at 1100℃ for 10 h.

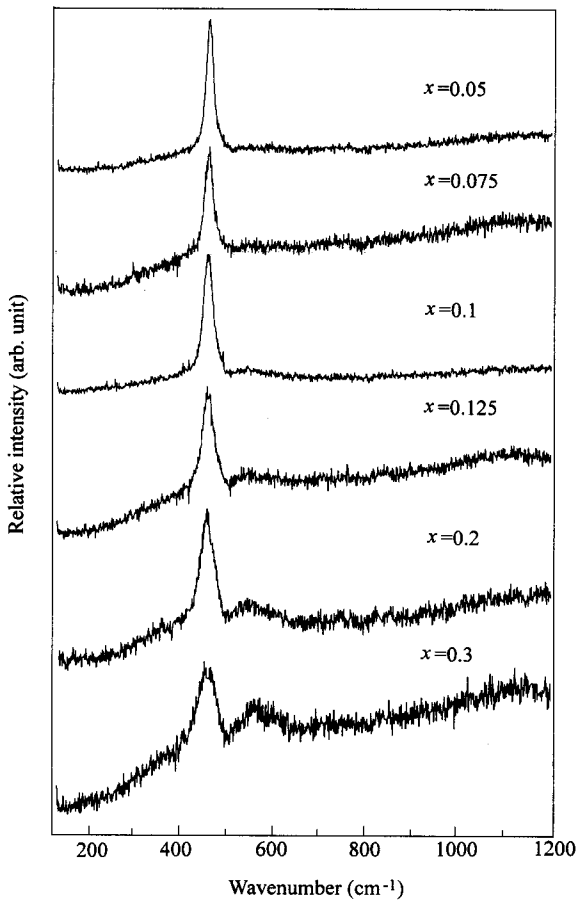

Fig. 4 Raman spectra of typical $Ce_{1-x}Nd_xO_{2-\delta}$ ($x = 0.05$—0.30) solid solution.

shift of the F_{2g} mode for our solid solutions.

The ionic conductivity of the solid solutions was measured by ac impedance spectroscopy. All impedance diagrams of the solid solutions consisted of two distinct semicircles (Fig. 5). The larger depressed semicircle at higher frequency was due to the bulk effect, while the smaller one at lower frequency was ascribed to the grain boundary conduction.[13] Fig. 5 shows typical impedance plot for the solid solution $Ce_{0.80}Nd_{0.20}O_{2-\delta}$ measured at 500 ℃. The intersection of the semicircles with the real part of the impedance (Z') axis was taken to determine the bulk and gain boundary resistance. Here we emphasized the bulk conduction. The temperature dependence of the bulk conductivity for solid solutions was shown in Fig. 6. It is clear that the bulk conductivity data for these solid solutions gave only one linear region and exhibited Arrhenius behavior over the temperature region, showing primarily oxide ion conduction. The ionic conductivities of $Ce_{1-x}Nd_xO_{2-\delta}$ solutions at 500 ℃ are 1.08 $\times 10^{-3}$, 1.14×10^{-3}, 2.65×10^{-3}, 0.503×10^{-3}, 0.325×10^{-3}, 0.011×10^{-3} S/cm for $x = 0.05$, 0.1, 0.2, 0.3, 0.35, and 0.4, respectively. That is, ionic conductivity increased gradually with increasing Nd substitution, reached a maximum at $x = 0.2$, and then decreased. The activation energy for the solution with $x = 0.2$ was 0.82 eV, which was much lower than that for undoped ceria.[2] It is clear that some amount of Nd_2O_3 doped in ceria lattice would produce considerable amount of extrinsic vacancy which significantly enhance the ionic conduction within the solid solutions. At a lower composition, the amount of oxygen vacancies increased with x, and therefore the conductivity increased. When composition is larger than $x = 0.2$, the higher concentration of oxygen vacancies would be accompanied by formation of defect associations $\{Nd_{Ce}V_O\}$ which reduces the relative

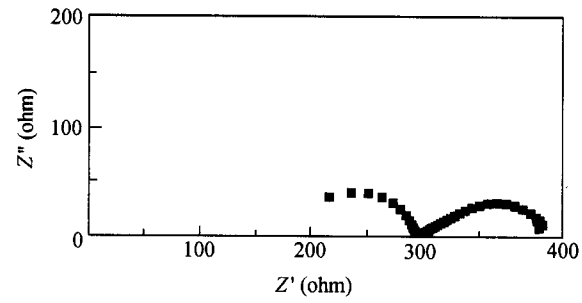

Fig. 5 Impedance spectra measured at 500℃ for sintering the dry gel at 1100℃ for 10 h.

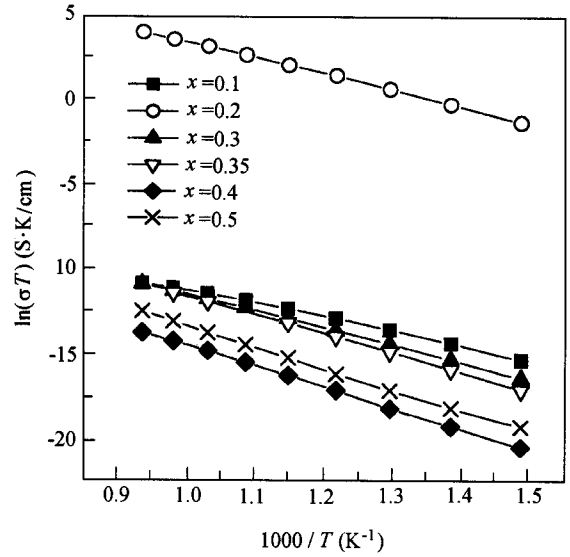

Fig. 6 Temperature dependence of the ionic conductivity for $Ce_{1-x}Sm_xO_{2-x/2}$ solid solutions.

content of effective oxygen vacancies for oxide ion hopping. Therefore, the conductivity decreased for the solid solutions with higher composition. Similar trends have been found in the $Ce_{1-x}Sm_xO_{2-x/2}$ and $Ce_{1-x}Ca_xO_{2-x}$ solid solutions.[3]

References

1 Inaba, H.; Tagawa, H. *Solid State Ionics* **1996**, *83*, 1.

2 Li, G. S.; Mao, Y. C.; Li, L. P.; Feng, S. H.; Wang, M. Q.; Yao, X. *Chem. Mater.* **1999**, *11*, 1259.

3 Huang, W.; Shuk, P.; Greenblatt, M. *Chem. Mater.* **1997**, *9*, 2240.

4 Abi-aad, E.; Bechara, R.; Grimblot, J.; Aboukais, A. *Chem. Mater.* **1996**, *5*, 793.

5 Shannon, R. D. *Acta Crystallogr., Sect. A: Found. Crystallogr.* **1976**, *32*, 751.

6 Li, L. P.; Li, G. S.; Che, Y. L.; Su, W. H. *Chem. Mater.* **2000**, *12*, 2567.

7 Bevan, D. J. M.; Summerville, E. ; Gschneider, K. A.; Eyring, L. *Handbook on the Physics and Chemistry on Rare Earth's*, Vol. 4, North Holland, Amsterdam, **1979**, p. 142.

8 Mogensen, M. ; Sammes, N. M.; Tompsett, G. A. *Solid State Ionics* **2000**, *129*, 63.

9 Shuk, P.; Greenblatt, M.; Croft, M. *J. Alloys Compd.* **2000**, *303*, 465.

10 Weber, W. H.; Hass, K. C.; McBride, J. R. *Phys. Rev. B: Condens. Matter* **1993**, *48*, 178.

11 McBride, J. R.; Hass, K. C.; Poindexter, B. D.; Weber, W. H. *J. Appl. Phys.* **1994**, *76*, 2435.

12 Keramidas, V. G.; White, W. B. *J. Chem. Phys.* **1973**, *59*, 751.

13 Li, G. S.; Li, L. P.; Feng , S. H. *Adv. Mater.* **1999**, *11*, 146.

(E200008173 LI, L.T.; DONG, L.J.)